A Reaction-Diffusion Model for Interference in Meiotic Crossing Over

Youhei Fujitani,*,[1] Shintaro Mori† and Ichizo Kobayashi‡

**Department of Applied Physics and Physico-Informatics, Faculty of Science and Technology, Keio University, Yokohama 223-8522, Japan, †Department of Physics, Faculty of Science, Kitasato University, Sagamihara, 228-8555, Japan and ‡Division of Molecular Biology, Institute of Medical Science, University of Tokyo, Tokyo 108-8639, Japan*

Manuscript received September 4, 2001
Accepted for publication February 1, 2002

ABSTRACT

One crossover point between a pair of homologous chromosomes in meiosis appears to interfere with occurrence of another in the neighborhood. It has been revealed that Drosophila and Neurospora, in spite of their large difference in the frequency of crossover points, show very similar plots of coincidence—a measure of the interference—against the genetic distance of the interval, defined as one-half the average number of crossover points within the interval. We here propose a simple reaction-diffusion model, where a "randomly walking" precursor becomes immobilized and matures into a crossover point. The interference is caused by pair-annihilation of the random walkers due to their collision and by annihilation of a random walker due to its collision with an immobilized point. This model has two parameters—the initial density of the random walkers and the rate of its processing into a crossover point. We show numerically that, as the former increases and/or the latter decreases, plotted curves of the coincidence *vs.* the genetic distance converge on a unique curve. Thus, our model explains the similarity between Drosophila and Neurospora without parameter values adjusted finely, although it is not a "genetic model" but is a "physical model," specifying explicitly what happens physically.

EARLY in meiosis, each pair of homologs comes together to form a tetrad containing two pairs of sister chromatids (Alberts *et al.* 1994; Zickler and Kleckner 1999; Figure 1a). The homologous recombination can occur between a pair of homologous regions, scattered along a pair of homologs, to cause a physical exchange of chromosomal parts between a pair of chromatids (Leach 1996). A resultant crossover point (or a chiasma) appears to suppress occurrence of another in the neighborhood, as was first observed in Drosophila (Sturtevant 1915; Muller 1916; Stahl 1979). Understanding how this genetic interference occurs would help not only in elucidating molecular details of genetic recombination and organization of genetic material but also in interpreting the vast amounts of data of human and other linkage analyses, for which a model supposing no interference, *i.e.*, the Poisson model proposed by Haldane (1919), is still widely used (Goldstein *et al.* 1995; McPeek and Speed 1995; Lin and Speed 1999).

Interference between two "points," or two short enough regions to be precise, disjoined along the chromosome is conventionally measured by the ratio of frequency of simultaneous crossing over at the two points to a product of crossing-over frequency at one of the points and that at the other (Weinstein 1936; Stahl 1979, p. 12; Foss *et al.* 1993; McPeek and Speed 1995); this ratio is called coincidence (for four-factor cross). Coincidence equals unity when no interference appears, *i.e.*, when crossover points occur independently of each other. When crossing over at one of the points suppresses occurrence of crossing over at the other, the frequency of simultaneous crossing over becomes smaller than expected for the case of no interference. Coincidence smaller than unity thus implies positive interference. Coincidence usually depends on the interval between the two points. The interval length is usually measured by the genetic distance (in morgans), which is defined as one-half the average number of crossover points occurring between the two points (Stahl 1979, p. 9; McPeek and Speed 1995).

Positive interference is explicit; *i.e.*, the coincidence drops to almost zero as the genetic distance becomes small, in datasets of *Drosophila melanogaster* with a 1.8×10^7 bp-long genome in three chromosomes per haploid (Morgan *et al.* 1935) and of *Neurospora crassa* with a 4.7×10^6 bp-long genome in seven chromosomes per haploid (Strickland 1961; Perkins 1962). As shown later, the overall appearance in this plot is very similar between these two organisms, in spite of the large difference in the frequency of crossover points (Foss *et al.* 1993).

The interference should come from some interaction between crossover points and/or their precursors, as was assumed in various models (McPeek and Speed 1995). Assuming that initial events, or intermediates, are distributed randomly and that every $(m + 1)$st event results in a crossover point, Foss *et al.* (1993) proposed a genetic model—a generalized version of a model by

[1]*Corresponding author:* Department of Applied Physics and Physico-Informatics, Faculty of Science and Technology, Keio University, Yokohama 223-8522, Japan. E-mail: youhei@appi.keio.ac.jp

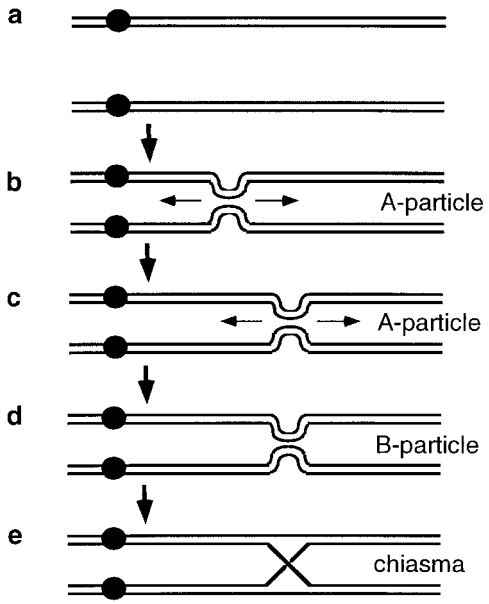

FIGURE 1.—Steps supposed in our model. (a) Each chromosome in a pair of homologs is replicated before meiosis. Each line represents a double-stranded DNA. A solid circle represents a centromere. (b) A contact point (an *A*-particle) occurs between a pair of homologous regions to help the homologs approach each other. (c) A contact point is thought to induce a second contact point at a neighboring homologous region. We simply regard this movement as random walk. (d) A contact point would become immobile. We refer to a contact point in this state as a *B*-particle. (e) A *B*-particle is assumed to be destined for a crossover point.

MORTIMER and FOGEL (1974). In this genetic model, where interaction is defined so that the interference is given by an immediate function of the genetic distance, the similarity is not derived from what is assumed but is assumed in itself. It follows in this model that no arbitrary adjustment of parameter values is required to explain the similarity between the two organisms.

The genetic model is equivalent to the chi-square model or the gamma model with the shape parameter $m + 1$ (FOSS *et al.* 1993; MCPEEK and SPEED 1995) and thus gives a biological basis to this mathematical model, providing good fits to data (MCPEEK and SPEED 1995; ZHAO *et al.* 1995a). The genetic model, however it may be expedient in fitting, does not specify the molecular mechanism of the interference by itself. Further modeling of how some machinery counts the number of intermediates and chooses the $(m + 1)$st one would require introduction of additional parameter(s). It would not be a simple problem to keep the additional parameter(s) still away from arbitrary adjustment in explaining the similarity.

We can model a molecular mechanism explicitly by defining the interaction in terms of a physical distance, as is usual in the physical sciences. The physical distance may be base pairs or micrometers, for example, depending on where and how the interaction is mediated. The interference would be given by an immediate function of the physical distance. The average number of resultant crossover points would give the relationship between the physical distance and the genetic distance; an interval with a given physical distance has a smaller genetic distance as crossover points become less frequent. FOSS *et al.* (1993) referred to a model with interaction defined in terms of a physical distance as a physical model.

KING and MORTIMER (1990) speculated that an immobile precursor (*e.g.*, an early nodule) is transformed stochastically into a structure doomed to be a crossover point (*e.g.*, a late nodule) and that hypothetical polymers then extend from the structure to eject flanking precursors. The polymer may be related to the Zip1 protein located in the central region of the synaptonemal complex (SYM and ROEDER 1994; ROEDER 1997). A modified version of this physical model (KING and MORTIMER 1990), supposing termination of polymer growth in addition, turned out to yield a good fit to the dataset of Drosophila in multilocus linkage analysis (MCPEEK and SPEED 1995). FOSS *et al.* (1993) claimed that rather arbitrary adjustments of parameter values are required in these physical models to explain the similarity between the difference organisms.

A physical model free from such adjustment could describe well the molecular mechanism for the similarity and provide a clue to the elementary process underlying the interference. We here propose a simple physical model, supposing a one-dimensional reaction-diffusion mechanism (or supposing diffusive and reactive particles in one dimension), inspired by a recent finding of premeiotic unstable contact points between intact duplexes of a pair of homologs (WEINER and KLECKNER 1994; ZICKLER and KLECKNER 1999). It is shown numerically that automatic adjustment works in our model to keep the same appearance in the plot of coincidence *vs.* genetic distance over a wide range of parameter values. Thus, the similarity is not assumed but derived without parameter values adjusted finely in this physical model. A preliminary report of this study was presented in a conference (FUJITANI *et al.* 2000).

MODEL

It is probable that, at the premeiotic stage or at the early stage of meiosis, local contact points appear between intact duplexes of a pair of homologs, each searching for a homologous region where homologous recombination is initiated. A contact point is imagined to be held by weak noncovalent interaction and to induce another in the neighborhood (Figure 1), which enables a one-dimensional search along the pair of homologs. The search could be much less efficient otherwise.

We assume this contact point to be a one-dimensional random walker along the pair of homologs (Figure 1, b and c). This assumption is not eccentric, considering that the Brownian motion along a biopolymer has been suggested in various systems, such as myosin along actin

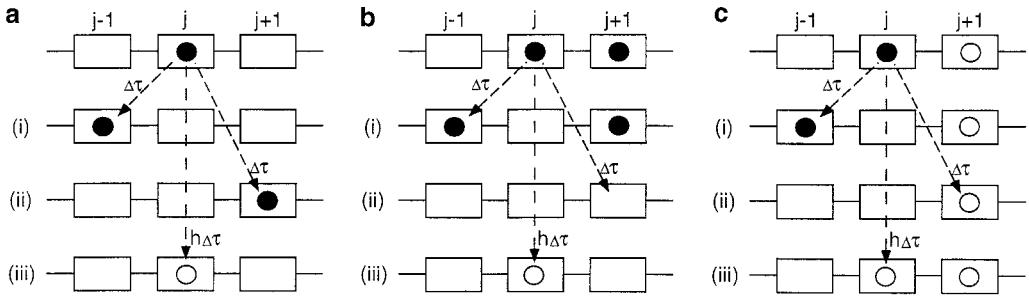

FIGURE 2.—Reaction-diffusion model. ●, *A*-particle; ○, *B*-particle. (a) A solid circle in a box at the top represents an *A*-particle at a lattice-site *j*. A dashed arrow represents a transition, by which the transition probability in an infinitesimal time interval $\Delta\tau$ is accompanied; we use a timescale so that a transition rate to (i) or to (ii) is unity. The *A*-particle shifts to the site $j-1$ with a probability $\Delta\tau$, shifts to the site $j+1$ with a probability $\Delta\tau$, and turns into a *B*-particle [an open circle in (iii)] with a probability $h\Delta\tau$ in this time interval. Mathematical details are described in the APPENDIX. (b) An *A*-particle undergoes the same transitions as shown in a even if another *A*-particle is at a next site. However, double occupancy is immediately followed by pair annihilation, as shown by (ii). (c) An *A*-particle undergoes the same transitions as shown in a even if an immobile *B*-particle is at a next site. However, double occupancy is immediately followed by annihilation of only the *A*-particle, as shown by (ii).

(ISHIJIMA *et al.* 1994), RNA polymerase along DNA (KABATA *et al.* 1993), and branch migration in homologous recombination (THOMPSON *et al.* 1976; FUJITANI *et al.* 1995; FUJITANI and KOBAYASHI 1999). A randomly walking contact point, which is below called an *A*-particle, would become immobile to be destined for a crossover point between one of the four possible pairs of the nonsister chromatids. Calling this immobile point a *B*-particle, we symbolize this immobilization with "$A \rightarrow B$" (Figure 1, c and d). No *B*-particles are there initially; *A*-particles are assumed to be produced at random along a pair of homologs only at the initial time.

Because of supposed instability, two *A*-particles would be annihilated pairwise when they collide ($A + A \rightarrow \varnothing$), and only an *A*-particle would be annihilated when it collides with a *B*-particle ($A + B \rightarrow B$), as shown schematically in Figure 2 and described in detail in the APPENDIX. As shown later, these interactions cause positive interference, *i.e.*, negative correlation of the *B*-particle density after a long enough time, when all the *A*-particles have disappeared. Our physical distance can be defined along the pair of homologs, where the random walker moves to mediate the interaction. Assuming that the random walk occurs over discrete lattice sites, we refer to the number l for two sites j and $j + l$ as the physical distance between them (Figure 2). This distance could not be related simply to the distance measured by the base pair; the number of base pairs corresponding with one step of the random walker depends on its location along the chromosome because the DNA molecule is packaged along the chromosome in a complex manner. We impose the periodic boundary condition for simplicity, as discussed in the APPENDIX.

We use a timescale so that the transition rate of the random walk is unity; results after a long enough time cannot be altered by use of any timescale. Prohibiting the simultaneous presence of more than one particle at a site ("exclusion principle"), we have two parameters α and h; the former denotes the initial average number of the *A*-particle per lattice site, and the latter denotes the transition rate of $A \rightarrow B$. As mentioned in the APPENDIX, we indicate the average over samples with $\langle \ldots \rangle$ in our stochastic model and write n_j for the final number of *B*-particles at site j. Its average $\langle n_j \rangle$ is independent from j because the governing rule [or (A1) in the APPENDIX], the initial condition, and the boundary condition make the system homogeneous. This independence does not necessarily contradict the occurrence of recombination hotspots (HABER 1997) because our physical distance cannot be related simply to the distance measured by the base pair. The genetic distance (in morgans) is defined as

$$g_l \equiv l\langle n_j \rangle/2, \tag{1}$$

where l is the physical distance with the unit being one random walker's step. The factor $\frac{1}{2}$ comes because two of the four chromatids are involved in each crossover point (STAHL 1979, p. 9; MCPEEK and SPEED 1995). The final correlation function of *B*-particles, given by $\langle n_j n_{j+l} \rangle$, *i.e.*, the average of a product of the final *B*-particle numbers at two sites, depends not on site j but on the interval length l. The coincidence can be expressed by

$$S_l \equiv \langle n_j n_{j+l} \rangle / (\langle n_j \rangle)^2, \tag{2}$$

as discussed by FOSS *et al.* (1993) and MCPEEK and SPEED (1995).

RESULTS

Plots against the physical distance: We obtain (1) and (2) numerically; details of our procedure are described in the APPENDIX. The S_l values are plotted against the physical distance l in Figure 3, a and b, where α is fixed to be 0.1 and 0.03, respectively. We find that interference extends to a larger physical distance as h (the rate of $A \rightarrow B$) decreases. Comparing results for the same h values in Figure 3, a and b, we also find that interference extends to a larger physical distance as α (the initial *A*-particle density) decreases. These tendencies are rea-

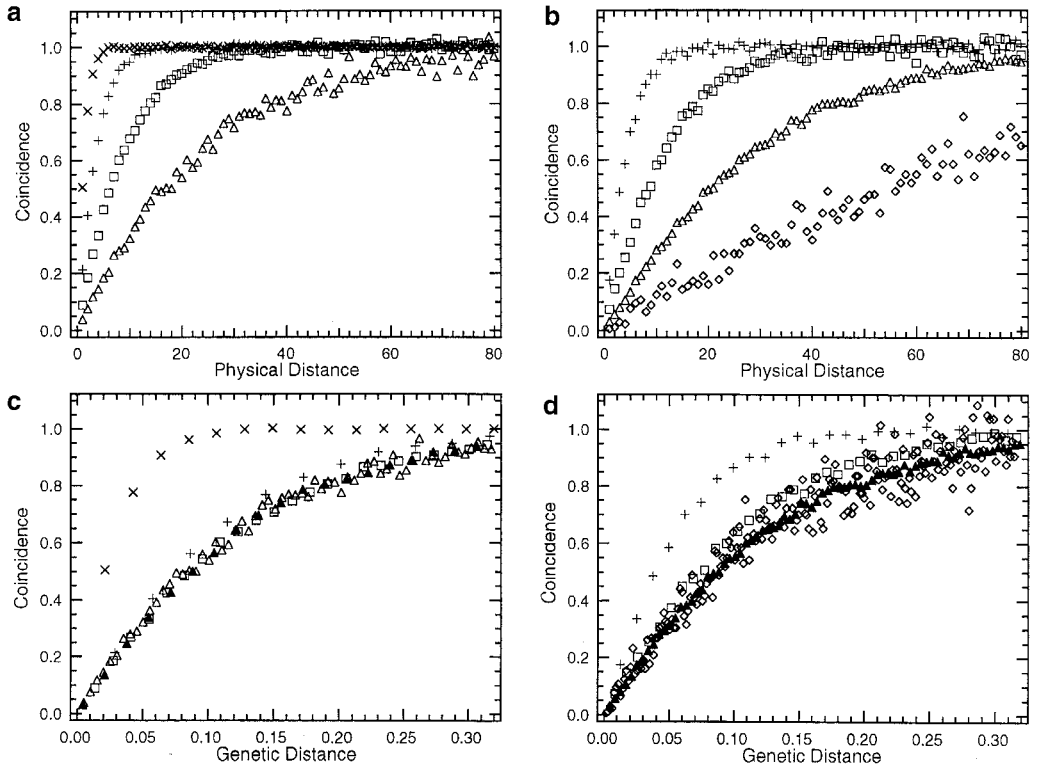

FIGURE 3.—Numerical results. Coincidence S_l is numerically calculated in our model; the final *B*-particle densities $\langle n_j \rangle$ are given in Table 1. We used 10^4 lattice sites and used 10^3 samples except 5×10^4 samples for (α, h) = (0.03, 0.001) and 2×10^5 samples for (0.03, 0.0001). (a) Cases of α = 0.1; results are plotted against the physical distance l. The h values are 0.001 (△), 0.01 (□), 0.1 (+), and 1.0 (×). (b) Cases of α = 0.03; results are plotted against the physical distance l. The h values are 0.0001 (◇), 0.001 (△), 0.01 (□), and 0.1 (+). (c) Results shown in a are replotted against the genetic distance g_l; the same symbols are used as in a. For comparison, results of (α, h) = (0.03, 0.001) are also plotted with solid triangles, which appear on a curve together with triangles and squares. (d) Results shown in b are replotted against the genetic distance g_l. The h values are 0.0001 (◇), 0.001 (▲), 0.01 (□), and 0.1 (+). Results for h = 0.0001 (◇) and for h = 0.001 (▲) cluster around the same curve on average, although fluctuations in the former results are rather large, in particular for larger g_l values.

sonable because an *A*-particle, mediating the interference, can survive longer as it turns to a *B*-particle less frequently and as it collides with another *A*-particle less frequently. Table 1 shows results of the final *B*-particle density $\langle n_j \rangle$, which decreases as h (the rate of $A \rightarrow B$) decreases and as α (the initial *A*-particle density) decreases, as expected.

Convergence in plots against the genetic distance: We replot the S_l values against the genetic distance g_l. When α = 0.1 (symbols other than solid triangles in Figure 3c), results converge on a limit curve as h decreases. Convergence is also found when α = 0.03 (Figure 3d). We should set h to be smaller to obtain the limit curve when α = 0.03 than when α = 0.1, which suggests that the convergence is slower as α decreases. Solid triangles in Figure 3, c and d, represent the same results for α =

TABLE 1

Final *B*-particle density

h	α = 0.003	α = 0.03	α = 0.1	α = 0.3
0.0001		3.1×10^{-3} (◇ in Figure 3, b and d)		
0.001	2.4×10^{-3} (× in Figure 5, a and b)	8.4×10^{-3} (△ in Figure 3b; ▲ in Figure 3, c and d; + in Figure 5, a and b)	1.0×10^{-2} (△ in Figure 3, a and c; ◇ in Figure 4, a and b)	1.1×10^{-2} (□ in Figure 5, a and b)
0.01		1.7×10^{-2} (□ in Figure 3, b and d)	2.7×10^{-2} (□ in Figure 3, a and c)	
0.1		2.5×10^{-2} (+ in Figure 3, b and d)	5.8×10^{-2} (+ in Figure 3, a and c)	
1.0			8.5×10^{-2} (× in Figure 3, a and c)	

Each item gives the final *B*-particle density for parameter values shown in the top row and in the extreme left column. Corresponding symbols and figure numbers are also given in parentheses.

0.03; comparison of solid triangles with other symbols in Figure 3c shows that the limit curves for $\alpha = 0.1$ and 0.03 are indistinguishable. It is thus suggested that results converge on the unique limit curve as h decreases, irrespective of the α-value. As h decreases with α fixed, crossover points becomes less frequent to shrink the genetic distance, and at the same time an A-particle survives longer to extend the suppression to a larger physical distance (Figure 3, a and b). The automatic adjustment thus works, and these counteractions balance to yield the limit curve. The coincidence curve keeps the same shape over a wide range of parameter values when it is plotted against the genetic distance.

Limit curve: Judging from Figure 3, c and d, $1 - S_l$ appears to decay exponentially as g_l increases. To verify this, we calculate

$$F_l \equiv -\ln(1 - S_l) \tag{3}$$

by use of S_l values on the limit curve and plot F_l values thus obtained numerically against g_l in Figure 4a (◇). As S_l tends to unity, a small error in it causes a large error in F_l because of the logarithm in (3); more scattered distribution of the data points (◇) for larger g_l values would be inevitable in Figure 4a. We can fit a line to the data points considering the above and find that the limit curve is expressed approximately by

$$S_l = 1 - \exp[-g_l/\xi]. \tag{4}$$

The correlation length ξ represents a typical genetic distance required to raise the curve appreciably and is given by the inverse of the slope of the line in Figure 4a. Curve fitting by use of the software IGOR (WaveMetrix, Lake Oswego, OR) yields $\xi = 0.118 \pm 0.001$ M (Figure 4b), where the number just after ± implies the standard deviation.

Comparison with observations: In Figure 4b, open and solid circles represent the data of Drosophila (Morgan *et al.* 1935), while crosses and asterisks represent the data of Neurospora (Strickland 1961; Perkins 1962). Coincidence almost vanishes in Drosophila when the genetic distance $< \sim 0.15$ morgans (Weinstein 1959). This initial lag appears a little bit smaller in Neurospora, as discussed in Foss *et al.* (1993), although it is not so explicit as in Drosophila (Figure 4b). Our model cannot explain this initial lag, unlike the genetic model, judging from curves with various parameter values shown in Figure 3; overall agreements with these datasets are thus clearly better in the genetic model, as shown by Figures 4 and 5 in Foss *et al.* (1993).

However, apart from this initial lag, our model can explain the datasets, as shown below. Plotting F_l by use of these data (Figure 4a), we find that data points of Drosophila for $g_l > \sim 0.15$ M (solid circles) can be fitted to a line. Thus, we can express approximately the coincidence beyond the short range by

$$S_l = 1 - \exp[-(g_l - g^{(0)})/\xi]. \tag{5}$$

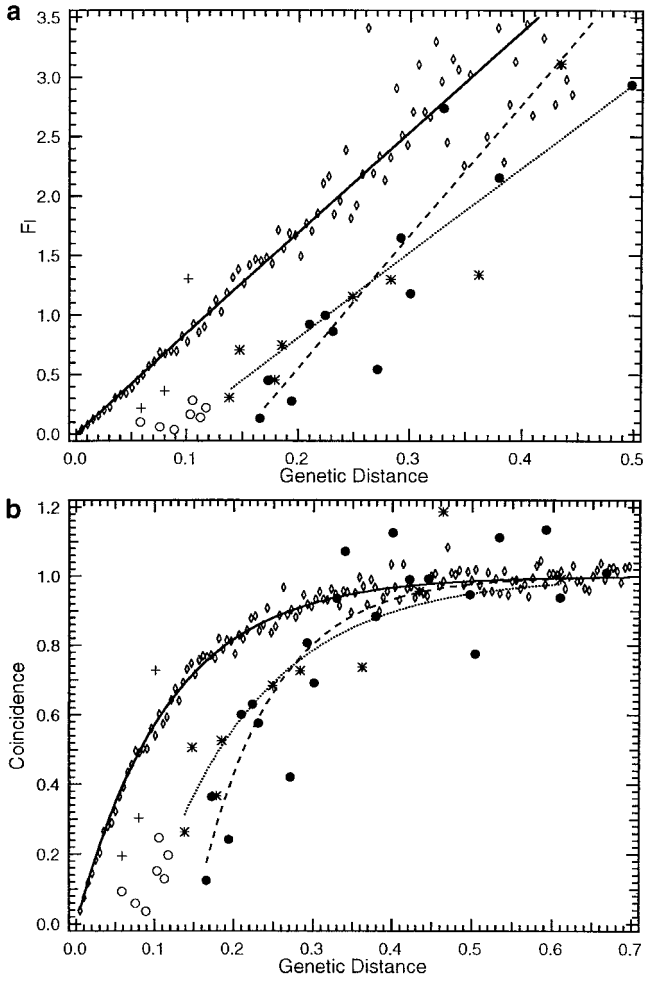

Figure 4.—Comparison with experimental data. (a) Calculating F_l by use of numerical results of $(\alpha, h) = (0.1, 0.001)$; *i.e.*, on the limit curve in Figure 3c, we plot F_l against g_l (◇). Solid and open circles represent data of Drosophila (Morgan *et al.* 1935), while crosses and asterisks represent data of Neurospora (Strickland 1961; Perkins 1962). These data points are from figures of Foss *et al.* (1993). Solid circles and asterisks, data points of $g_l \geq 0.13$ M, are used in curve fitting done in b. Lines are replots of corresponding fitted curves obtained in b. (b) Coincidence S_l is plotted against the genetic distance g_l. Results of $(\alpha, h) = (0.1, 0.001)$ are replotted (◇), as in Figures 3c and 4a. Curve fitting of (4) to the numerical results yields a solid curve with $\xi = 0.118 \pm 0.001$ M. The experimental data are also plotted by use of the same symbols as in a. Curve fitting of (5) to the solid circles yields a dashed curve with $\xi = 0.09 \pm 0.02$ M and $g^{(0)} = 0.15 \pm 0.01$ M. Curve fitting of (5) to the asterisks yields a dotted curve with $\xi = 0.14 \pm 0.04$ M and $g^{(0)} = 0.09 \pm 0.03$ M.

Curve fitting yields $\xi = 0.09 \pm 0.02$ M and $g^{(0)} = 0.15 \pm 0.01$ M (Figure 4b). Data points of Neurospora in Figure 4a can also be fitted to a line for $g_l > \sim 0.13$ M (asterisks); the coincidence can be also expressed by (5). Curve fitting yields $\xi = 0.14 \pm 0.04$ M and $g^{(0)} = 0.09 \pm 0.03$ M (Figure 4b). Thus the fitted values of ξ, *i.e.*, the correlation length measured by the genetic distance, for the limit curve, for the data of Drosophila and for the data of Neurospora, agree, considering their confidence

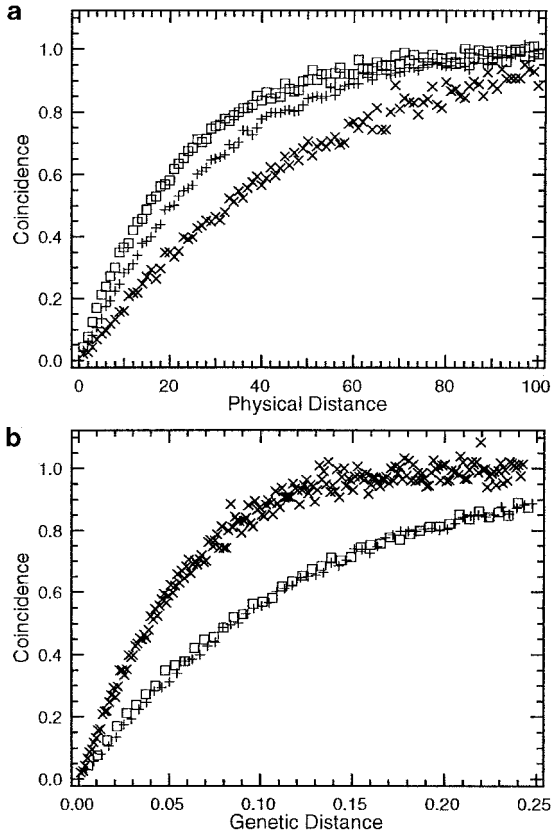

FIGURE 5.—Dependence on the initial density. Coincidence S_l is obtained numerically when $h = 0.001$. We used 10^4 lattice sites and 5×10^4 samples, except for 5×10^3 samples for $\alpha = 0.3$. (a) Results are plotted against the physical distance l. The α values are 0.3 (□), 0.03 (+), and 0.003 (×); the final B-particle densities are given in Table 1. Crosses are replots of triangles in Figure 3b. (b) Results in a are replotted against the genetic distance g_l. The same symbols are used as in a. Crosses are replots of solid triangles in Figure 3d.

intervals. Thus, our model can explain the observed correlation length, *i.e.*, how the observed coincidence increases as the genetic distance increases beyond a range of the initial lag.

Dependence on the initial density: Comparing crosses in Figure 3c ($h = \alpha = 0.1$) with those in Figure 3d ($h = 0.1$ and $\alpha = 0.03$), we can expect that the convergence also appears as α increases with h fixed. We here show this explicitly. Plotting numerical results of coincidence against the physical distance for a fixed h value, we find that the correlation length measured by the physical distance becomes larger as α decreases (Figure 5a). Replotting the results against the genetic distance, we explicitly find that they converge on a limit curve as α increases. Considering that crosses in Figure 5b are replots of solid triangles in Figure 3, c and d, results appear to converge on the unique limit curve as α increases with h fixed or as h decreases with α fixed. When h is fixed to be so large, we cannot increase α enough to obtain the limit curve (data not shown) because the exclusion principle demands $\alpha \leq 1$. The results for $\alpha = 0.003$ are lowermost in Figure 5a, while they are uppermost in Figure 5b, because smaller α makes crossover points less frequent to shrink the genetic distance.

DISCUSSION

It is thought that an unstable premeiotic contact point identified by WEINER and KLECKNER (1994) occurs between intact duplexes because its occurrence usually precedes that of meiosis-specific double-strand breaks (DSBs). Probably DSBs occur in early nodules associated with the axial elements (BISHOP 1994; ANDERSON *et al.* 1997) and prime homologous recombination. A relationship between the contact point and the DSB has not yet been established although the axial element may play a role in relating them (KLECKNER 1997, p. 35; ZICKLER and KLECKNER 1999, p. 677). The axial element is integrated into the synaptonemal complex (SC); the late nodule in the central region of the SC shows a convincing correlation with the following crossover point (CARPENTER 1975; ZICKLER and KLECKNER 1999).

Schizosaccharomyces pombe and *Aspergillus nidulans* fail to form SCs and show no positive interference (EGEL-MITANI *et al.* 1982; BAHLER *et al.* 1993). Mutant studies also suggest a relationship between SC formation and occurrence of positive interference (JONES 1967; SYM and ROEDER 1994; ROEDER 1997). It has not yet been established, however, whether the latter requires the former or some proteins (*e.g.*, Zip1) contribute to both (STORLAZZI *et al.* 1996).

Many details of the molecular mechanism of meiosis thus remain to be elucidated experimentally. At this stage, it would be rather hard to evaluate a model requiring fine adjustment of parameter values to explain observations. It is thus of interest to search for a model explaining the similarity between the datasets of Drosophila and Neurospora without fine adjustment of parameter values. Analyzing these datasets, showing positive interference explicitly, would lead to understanding the elementary mechanism underlying the interference. We also expect that the elementary process gives this similarity not by chance but inherently; *i.e.*, the similarity would result not because each organism has special parameter values but because its appearance in the plot is insensitive to parameter values of the elementary process.

Inspired by recent findings of premeiotic contact points (WEINER and KLECKNER 1994; ZICKLER and KLECKNER 1999), we have formulated the process in terms of a one-dimensional reaction-diffusion model with $A \to B$, $A + A \to \emptyset$, and $A + B \to B$, where B-particles are immobile. Our model is a kind of physical model because it supposes a random walk defined in terms of a physical distance. Although our A-particle could be a premeiotic contact point identified by WEINER and KLECKNER (1994) or an early nodule, other possibilities can never be excluded at this stage.

In our model, as h (the rate of $A \rightarrow B$) decreases with α (the initial A-particle density) fixed, a contact point survives longer to extend the interference to a larger physical distance at the same time as when less frequent crossover points make the genetic distance shrink. These counteractions balance to yield the unique limit curve in the plot of coincidence *vs.* the genetic distance. The same convergence appears as α increases with h fixed to be small enough. Thus, our physical model has a nontrivial mechanism of automatic adjustment to keep the same appearance in this plot over a wide range of parameter values. Our limit curve has the correlation length in agreement with that observed in Drosophila and Neurospora. Our simple model is thus not only the first physical model that yields the similarity without parameter values adjusted finely but is also comparable with the experimental datasets quantitatively.

We believe that our study is meaningful because it shows that a simple physical model can yield similarity without parameter values adjusted finely. Our model will be improved so as to explain the initial lag in addition to the similarity. This would be possible after elucidating analytically how the convergence comes out in our model. The models of King and Mortimer (1990) are apparently different from our model because they supposed an immobile precursor and polymers growing with a constant rate to transmit interaction. However, mathematical comparison between this model (or other models) and our model will also be studied. Further, it will be studied whether or not our model for the elementary process may be modified to explain the absence of positive interference in some organisms.

We are grateful to Frank Stahl for comments on our manuscript. The work by Y.F. is partly supported by Keio Gakuji Shinko Shikin. The work by I.K. was supported by the Ministry of Education, Culture, Sports, Science and Technology of the Japanese government (Repair, Recombination and Genome), the New Energy and Industrial Technology Development Organization, and Uehara Memorial Foundation.

LITERATURE CITED

Alberts, B., D. Bray, J. Lewis, M. Raff, K. Roberts *et al.*, 1994 *Molecular Biology of the Cell*, Chap. 20. Garland, New York.

Anderson, L. K., H. H. Offenberg, W. M. H. C. Verkuijlen and C. Heyting, 1997 RecA-like proteins are components of early meiotic nodule in lily. Proc. Natl. Acad. Sci. USA **94:** 6868–6873.

Bahler, J., T. Wyler, J. Loidl and J. Kohli, 1993 Unusual nuclear structures in meiotic prophase of fission yeast. J. Cell Biol. **121:** 241–256.

Bishop, D. K., 1994 RecA homologs Dmc1 and Rad51 interact to form discrete nuclear complexes prior to meiotic chromosome synapsis. Cell **79:** 1081–1092.

Carpenter, A. T. C., 1975 Electron microscopy of meiosis in *Drosophila melanogaster* females. II. The recombination nodule—a recombination-associated structure at pachytene? Proc. Natl. Acad. Sci. USA **72:** 3186–3189.

Egel-Mitani, M., L. W. Olson and R. Egel, 1982 Meiosis in *Aspergillus nidulans*: another example for lacking synaptonemal complexes in the absence of crossover interference. Heredity **97:** 179–187.

Foss, E., R. Lande, F. W. Stahl and C. M. Steinberg, 1993 Chiasma interference as a function of genetic distance. Genetics **133:** 681–691.

Fujitani, Y., and I. Kobayashi, 1999 Effect of DNA sequence divergence on homologous recombination as analyzed by a random-walk model. Genetics **153:** 1973–1988.

Fujitani, Y., K. Yamamoto and I. Kobayashi, 1995 Dependence of frequency of homologous recombination on the homology length. Genetics **140:** 797–809.

Fujitani, Y., S. Mori and I. Kobayashi, 2000 Reaction-diffusion model for genetic interference, pp. 230–231 in *Currents in Computational Molecular Biology*, edited by S. Miyano, R. Shamir and T. Takagi. Universal Academy Press, Tokyo.

Goldstein, D. R., T. P. Speed and H. Zhao, 1995 Relative efficiencies of chi-square models of recombination for exclusion mapping and gene ordering. Genomics **27:** 265–273.

Haber, J. E., 1997 A super new twist on the initiation of meiotic recombination. Cell **89:** 163–166.

Haldane, J. B. S., 1919 The combination of linkage values and the calculation of distances between loci of linked factors. J. Genet. **8:** 299–309.

Holliday, R., 1964 A mechanism for gene conversion in fungi. Genet. Res. **5:** 282–304.

Ishijima, A., Y. Harada, H. Kojima, T. Funatsu, H. Higuchi *et al.*, 1994 Single-molecule analysis of the actomyosin motor using nanomanipulation. Biochem. Biophys. Res. Commun. **199:** 1057–1063.

Jones, G. H., 1967 The control of chiasma distribution in rye. Chromosoma **22:** 69–90.

Kabata, H., O. Kurosawa, I. Arai, M. Washizu, S. A. Margarson, R. E. Glass and N. Shimamoto, 1993 Visualization of single molecules of RNA polymerase sliding along DNA. Science **262:** 1561–1563.

King, J. S., and R. K. Mortimer, 1990 A polymerization model of chiasma interference and corresponding computer simulation. Genetics **126:** 1127–1138.

Kleckner, N., 1997 Interactions between and along chromosomes during meiosis, pp. 21–45 in *The Harvey Lectures, Series 91*. Wiley-Liss, New York.

Leach, D. R. F., 1996 *Genetic Recombination*. Blackwell Science, Oxford.

Lin, S., and T. P. Speed, 1999 Relative efficiency of the Chi-square recombination models for gene mapping with human pedigree data. Ann. Hum. Genet. **63:** 81–95.

McPeek, M. S., and T. P. Speed, 1995 Modeling interference in genetic recombination. Genetics **139:** 1031–1044.

Morgan, T. H., C. B. Bridges and J. Schultz, 1935 Constitution of the germinal material in relation to heredity. Carnegie Inst. Wash. Year Book **34:** 284–291.

Mortimer, R. K., and S. Fogel, 1974 Genetical interference and gene conversion, pp. 263–275 in *Mechanisms in Recombination*, edited by R. F. Grell. Plenum, New York.

Muller, H. J., 1916 The mechanism of crossing-over. Am. Nat. **50:** 193–221.

Perkins, D. D., 1962 Crossing-over and interference in a multiply-marked chromosome arm of Neurospora. Genetics **47:** 1253–1274.

Roeder, G. S., 1997 Meiotic chromosomes: it takes two to tango. Genes Dev. **11:** 2600–2621.

Stahl, F. W., 1979 *Genetic Recombination*. W. H. Freeman, San Francisco.

Storlazzi, A. L., L. Xu, A. Schwacha and N. Kleckner, 1996 Synaptonemal complex (SC) component Zip1 plays a role in meiotic recombination independent of SC polymerization along the chromosomes. Proc. Natl. Acad. Sci. USA **93:** 9043–9048.

Strickland, W. N., 1961 Tetrad analysis of short chromosome regions of *Neurospora crassa*. Genetics **46:** 1125–1141.

Sturtevant, A. H., 1915 The behavior of the chromosomes as studied through linkage. Z. Indukt. Abstammungs-Vererbungsl. **13:** 234–287.

Sym, M., and G. S. Roeder, 1994 Crossover interference is abolished in the absence of a synaptonemal complex protein. Cell **79:** 283–292.

Thompson, B. J., M. N. Camien and R. C. Warner, 1976 Kinetics of branch migration in double-stranded DNA. Proc. Natl. Acad. Sci. USA **73:** 2299–2303.

van Kampen, N. G., 1992 *Stochastic Processes in Physics and Chemistry*. Elsevier, Amsterdam.

Weiner, B. M., and N. Kleckner, 1994 Chromosome pairing via multiple interstitial interactions before and during meiosis. Cell **77:** 977–991.

Weinstein, A., 1936 The theory of multiple-strand crossing over. Genetics **21:** 155–199.
Weinstein, A., 1959 The geometry and mechanics of crossing over. Cold Spring Harbor Symp. Quant. Biol. **23:** 177–196.
Zhao, H., T. P. Speed and M. S. McPeek, 1995a Statistical analysis of crossover interference using the chi-square model. Genetics **139:** 1045–1056.
Zhao, H., T. P. Speed and M. S. McPeek, 1995b Statistical analysis of chromatid interference. Genetics **139:** 1057–1065.
Zickler, D., and N. Kleckner, 1999 Meiotic chromosomes: integrating structure and function. Annu. Rev. Genet. **33:** 603–754.

Communicating editor: N. Takahata

APPENDIX

Our model presupposes that no chiasma occurs between a pair of sister chromatids and that combination of nonsister chromatids exchanged at a chiasma never influences choice of chromatids at a nearby chiasma (no chromatid interference; Zhao *et al.* 1995b). For experimental data, we assume that the change of markers implies occurrence of crossing over, neglecting the possibility of homologous recombination just on the marker site.

Details of our model are as follows. The particle distribution over lattice sites 1, 2, . . . , N can be labeled by $\boldsymbol{x} = (x_1, x_2, \ldots, x_N)$, where x_j represents a state of a site j. Let us stipulate $x_j = 0$ if the site j is vacant, $x_j = 1$ if it is occupied by an A-particle, and $x_j = 2$ if it is occupied by a B-particle. The site 1 is next to the site N because the lattice is assumed to be periodic.

A set of distributions $\Omega_1(\boldsymbol{x})$ is defined so that we can turn a distribution $\boldsymbol{x}' \in \Omega_1(\boldsymbol{x})$ into the distribution $\boldsymbol{x}$ by shifting an A-particle from a site to a next site. This shift is shown by (i) and (ii) in Figure 2, a–c, and may result in particle annihilation. Conversely, a set $\Omega_2(\boldsymbol{x})$ is defined so that we can turn $\boldsymbol{x}$ into $\boldsymbol{x}' \in \Omega_2(\boldsymbol{x})$ by this shift of an A-particle. A set $\Omega_3(\boldsymbol{x})$ is defined so that we can turn a distribution $\boldsymbol{x}' \in \Omega_3(\boldsymbol{x})$ into $\boldsymbol{x}$ by changing an A-particle into a B-particle at the site, as shown by (iii) in Figure 2. Conversely, a set $\Omega_4(\boldsymbol{x})$ is defined so that we can turn $\boldsymbol{x}$ into $\boldsymbol{x}' \in \Omega_4(\boldsymbol{x})$ by a transition $A \rightarrow B$. Let $P(\boldsymbol{x}, t)$ denote the probability of $\boldsymbol{x}$ at time t, and the master equation of our model is

$$\frac{\partial}{\partial t}P(\boldsymbol{x}, t) = D\left\{\sum_{\boldsymbol{x}'\in\Omega_1(\boldsymbol{x})} P(\boldsymbol{x}', t) - \sum_{\boldsymbol{x}'\in\Omega_2(\boldsymbol{x})} P(\boldsymbol{x}, t)\right\} + H\left\{\sum_{\boldsymbol{x}'\in\Omega_3(\boldsymbol{x})} P(\boldsymbol{x}', t) - \sum_{\boldsymbol{x}'\in\Omega_4(\boldsymbol{x})} P(\boldsymbol{x}, t)\right\}, \tag{A1}$$

where D and H are constants, denoting the transition rate of shifting an A-particle from a site to a next site and that of $A \rightarrow B$, respectively (van Kampen 1992). The initial distribution is assumed to be a binomial distribution: $P(\boldsymbol{x}, 0) = \alpha^m(1 - \alpha)^{N-m}$ if the set $\{x_1, x_2, \ldots, x_N\}$ has m elements equal to unity and has none equal to 2, and $P(\boldsymbol{x}, 0) = 0$ if the set contains an element equal to 2.

Let us introduce a nondimensionalized time $\tau \equiv Dt$; we can write the master equation in terms of $p(\boldsymbol{x}, \tau) \equiv P(\boldsymbol{x}, \tau/D)$ as

$$\frac{\partial}{\partial\tau}p(\boldsymbol{x}, \tau) = \sum_{\boldsymbol{x}'\in\Omega_1(\boldsymbol{x})} p(\boldsymbol{x}', \tau) - \sum_{\boldsymbol{x}'\in\Omega_2(\boldsymbol{x})} p(\boldsymbol{x}, \tau) + h\left\{\sum_{\boldsymbol{x}'\in\Omega_3(\boldsymbol{x})} p(\boldsymbol{x}', \tau) - \sum_{\boldsymbol{x}'\in\Omega_4(\boldsymbol{x})} p(\boldsymbol{x}, \tau)\right\}, \tag{A2}$$

where H/D coincides with h as defined in the text.

Let us define sets of distributions as $\Gamma_j = \{\boldsymbol{x}|x_j = 2\}$ and $\Gamma_{jk} = \{\boldsymbol{x}|x_j = x_k = 2\}$, and the expectation values defined in the text are

$$\langle n_j\rangle \equiv \sum_{\boldsymbol{x}'\in\Gamma_j} P(\boldsymbol{x}', \infty) = \sum_{\boldsymbol{x}'\in\Gamma_j} p(\boldsymbol{x}', \infty) \tag{A3}$$

$$\langle n_j n_k\rangle \equiv \sum_{\boldsymbol{x}'\in\Gamma_{jk}} P(\boldsymbol{x}', \infty) = \sum_{\boldsymbol{x}'\in\Gamma_{jk}} p(\boldsymbol{x}', \infty). \tag{A4}$$

Thus, we can start from (A2), instead of (A1), to obtain (1) and (2). A probability with which an A-particle undergoes one of the transitions, *i.e.*, shift to a next site or $A \rightarrow B$, in an infinitesimal time interval $\Delta\tau$ is $\Delta\tau + \Delta\tau + h\Delta\tau = (2 + h)\Delta\tau$, as found in Figure 2. When m A-particles are left on the lattice, we can expect that, on average, one of the A-particles undergoes a transition in a time interval $1/\{m(2 + h)\}$.

In our numerical study, we take this time interval for one calculation step, where we have only one transition of an A-particle. Suppose that a sample of the initial particle distribution is given. In one step, selecting an A-particle randomly, we shift it to the neighboring left site with a probability $1/(2 + h)$, shift it to the neighboring right site with a probability $1/(2 + h)$, and change it into a B-particle with a probability $h/(2 + h)$. Then, we may annihilate (an) A-particle(s) following the rules shown in Figure 2. After repeating this procedure, we obtain a sample of the final B-particle distribution when all the A-particles have disappeared. As in the text, we write n_j for the final number of B-particles at site j in a sample; we can obtain (A3) by averaging n_j over samples and obtain (A4) by averaging the product $n_j n_k$ over samples.

We previously proposed a model for homologous recombination, which also supposes one-dimensional random walk (Fujitani *et al.* 1995; Fujitani and Kobayashi 1999). This random-walk model is different, in the scale and contents, from our present model for genetic interference. It was assumed in the former model that one connecting point, such as a Holliday structure (Holliday 1964), walks randomly in one homologous region; its annihilation at either end explained observed nonlinear dependence of recombination frequency on the region's length. The present model supposes many interacting unstable contact points walking randomly over homologous regions and explains the similarity in meiotic recombination between the two organisms.